Journal of Organometallic Chemistry, 287 (1985) 305–320
Elsevier Sequoia S.A., Lausanne – Printed in The Netherlands

TRIS(TRIMETHYLSILYLAMINO)SILANES $RSi(NHSiMe_3)_3$. SYNTHESIS, CRYSTAL AND MOLECULAR STRUCTURE OF THREE DIMERIC TRILITHIO DERIVATIVES *

D.J. BRAUER, H. BÜRGER, G.R. LIEWALD and J. WILKE
Anorganische Chemie, Fachbereich 9, Universität-Gesamthochschule, D-5600 Wuppertal (F.R.G.)
(Received November 14th, 1984)

Summary

$MeSi(NHSiMe_3)_3$ (I) and $t\text{-}BuSi(NHSiMe_3)_3$ (II) have been prepared and their ^1H NMR, infrared and Raman spectra determined. Reaction of I, II and $PhSi(NHSiMe_3)_3$ with n-butyllithium yielded the respective trilithio derivatives VI, VII and VIII, for which ^1H and ^7Li NMR, infrared and Raman spectra are reported. Each trilithio derivative has been shown by X-ray diffraction to form dimers in the solid state. Ignoring the phenyl groups in VIII, the symmetry of the dimers approaches $\bar{3}m(D_{3d})$. The dimers may be described as a trigonal antiprismatic core of six lithium atoms to which two $RSi(NSiMe_3)_3$ fragments are attached. Each nitrogen and lithium atom forms three Li–N bonds, so that the bonding in the Li_6N_6 clusters is electron deficient. The relationship between these clusters and an undistorted icosahedron is discussed.

Introduction

The unique properties of the disilylamino ligand for the stabilization of unusual coordination numbers of main group elements [1] and transition metals [2] are well documented. Alkali metal derivatives $(R_3Si)_2NM$ play an important rôle as transfer reagents for R_3Si groups [2]. Since these alkali metal derivatives are often molecular rather than ionic species despite the presence of rather ionic bonding, numerous investigations of their structures have been reported [3–6].

Bis(triorganosilylamino)silanes (trisiladiazanes), $R_2Si(NHSiR_3)_2$ are known to exhibit many of the above-mentioned properties of the disilylamines. As a ligand the bis(silylamino)silyl group preferentially forms four-membered ring systems, $R_2Si(NSiR_3)_2X$, with main group and transition elements X. We recently described

* Dedicated to Professor Dr. mult. G. Wilke on the occasion of his 60th birthday on 23rd February 1985.

0022-328X/85/$03.30

the synthesis and crystal and molecular structure of the disodio derivative $(Me_3SiNNa)_2SiMe_2$ [7]. In the solid this species forms a trimer with a trigonal bipyramidal Na_6 cluster and unusually short Na...C contacts. The mode of aggregation of this sodium derivative is in contrast with the infinite chain structure of $(Me_3Si)_2NNa$ [6].

This paper deals with the potentially tridentate ligands $(R_3SiNH)_3SiR$ which, like (silylamino)silanes $(R_3SiNH)SiR_3$ and bis(silylamino)silanes $(R_3SiNH)_2SiR_2$, have SiNHSi functional groups. Though many tris(organoamino)silanes $(R'NH)_3SiR$ have been reported [2], only one example, $PhSi(NHSiMe_3)_3$ (III), containing the SiNHSi linkage has been mentioned [8–10]. We describe below the synthesis of two further examples, $MeSi(NHSiMe_3)_3$ (I) and $Me_3CSi(NHSiMe_3)_3$ (II), their metallation, and the structure of the three trilithiated silylamines $RSi(NLiSiMe_3)_3$, R = Me (VI), R = Me_3C (VII) and R = Ph (VIII).

Synthesis of amines

The reaction of organosilicon trihalides with primary amines (eq. 1) is the

$$RSiX_3 + 6R'NH_2 \rightarrow 3R'NH_3X + RSi(NHR')_3 \quad (1)$$

standard method for the synthesis of tris(organoamino)organosilanes. This reaction is however not suited for the preparation of tris(triorganosilylamino)(organo)silanes $RSi(NHSiR'_3)_3$.

Three different pathways have been described for the synthesis of III, the first reported isotetrasilatriazane:

(i) simultaneous ammonolysis of $PhSiCl_3$ and MeSiCl (eq. 2) [8]:

$$PhSiCl_3 + 3Me_3SiCl + 9NH_3 \rightarrow 6NH_4Cl + III \quad (2)$$

(ii) a three step synthesis according to eq. 3a–3c [9]:

$$PhSiCl_3 + 2(Me_3Si)_2NH \rightarrow 2Me_3SiCl + PhSi(Cl)(NHSiMe_3)_2 \quad (3a)$$

$$PhSi(Cl)(NHSiMe_3)_2 + 2NH_3 \rightarrow NH_4Cl + PhSi(NH_2)(NHSiMe_3)_2 \quad (3b)$$

$$PhSi(NH_2)(NHSiMe_3)_2 + Me_3SiCl + Et_3N \rightarrow Et_3NHCl + III \quad (3c)$$

(iii) treatment of $PhSiCl_3$ with $(Me_3Si)_2NH$ in the presence of pyridine (eq. 4) [10]:

$$PhSiCl_3 + 3(Me_3Si)_2NH \xrightarrow{C_5H_5N} 3Me_3SiCl + III \quad (4)$$

The yields of III were poor, viz. 8, 10 (overall yield) and 30% from the procedures (i), (ii) and (iii), respectively. Since the procedure shown in eq. 4 seemed to be the most convenient, we used it for the synthesis of III, and confirm the reported yield.

In order to study the influence of the R substituent in the $RSi(NHSiMe_3)_3$ series, we attempted to synthesize the methyl (I) and t-butyl derivative (II) according to eq. 2 and 4. Compound I was isolated, in yields of 5 and 17%, from reactions corresponding to 2 and 4, respectively, but the steric influence of the t-Bu group directs both reactions mainly to other products. In the presence of pyridine only one halogen atom of $t\text{-}BuSiCl_3$ was replaced by use of $(Me_3Si)_2NH$, and IV was obtained in 13% yield (eq. 5).

$$t\text{-}BuSiCl_3 + (Me_3Si)_2NH \xrightarrow{C_5H_5N} Me_3SiCl + t\text{-}BuSiCl_2NHSiMe_3 \quad (5)$$
(IV)

Simultaneous ammonolysis of t-$BuSiCl_3$ and Me_3SiCl gave V in 15% yield, eq. 6.

$$t\text{-}BuSiCl_3 + 2Me_3SiCl + 8NH_3 \rightarrow 5NH_4Cl + t\text{-}BuSi(NH_2)(NHSiMe_3)_2 \quad (6)$$
(V)

Compound V is a suitable precursor for II, which was obtained in 70% yield by the route shown in eq. 7.

$$V \xrightarrow[2.-LiCl]{\substack{1.+C_4H_9Li,\\ 2.+Me_3SiCl}} II \quad (7)$$

Properties

The physical properties of I to V are shown in Table 1. All are colourless liquids, soluble in polar and nonpolar organic solvents. The dichloride IV is particularly sensitive to moisture. Their formulation is confirmed by their ^1H NMR spectra. Infrared and Raman spectra are presented in the Experimental section, and diagnostic vibrations of the SiNHSi skeleton are listed in Table 1. The mass spectra (see Experimental), which show the $[M - CH_3]^+$ ions, are consistent with the assumed formulations; elimination of Me_3Si, Me, CH_4 and t-Bu are the main fragmentation steps.

Lithium silylamides

Lithiation of the silylamides I to III with n-butyllithium proceeds rapidly and completely at room temperature in non-polar solvents (eq. 8).

TABLE 1

PROPERTIES OF COMPOUNDS I TO V

	I	II	III	IV	V
B.p. (°C/Torr)	83/1	88/1	115/1	64–65/3	75/1
^1H NMR [a]					
$\delta(SiMe_3)$ (ppm)	0.14	0.12	0.08	0.10	0.10
δ(R) (ppm)	0.14	0.88	7.68/7.23	0.88	0.97
ν(NH) (cm^{-1})	3385	3380	3378	3373	3385
δ(SiNHSi) (cm^{-1})	1178	1177	1178	1180	1178
ν_{as}(SiNSi) (cm^{-1})	919	933	927	952	934
ν_s(SiNSi) (cm^{-1})	550	545			572
$\nu(NH_2)$ (cm^{-1})					3495/3461
$\delta(NH_2)$ (cm^{-1})					1542
ν(SiCl) (cm^{-1})				470/559	

[a] In C_6H_6, int. std. TMS.

$$RSi(NHSiMe_3)_3 + 3C_4H_9Li \rightarrow 3C_4H_{10} + RSi[N(Li)SiMe_3]_3 \quad (8)$$

(VI, R = Me; VII, R = t-Bu; VIII, R = Ph)

The trilithio compounds VI to VIII crystallize from the reaction solutions upon cooling. Yields of isolated material were of the order of 60%, though the metallation reaction 8 is essentially quantitative. Surprisingly, the reactivity of the NH function did not decrease with proceeding lithiation; this is in contrast to observations on metallation of $Me_2Si(NHSiMe_3)_2$ for which monometallated species were obtained exclusively upon initial treatment with n-butyllithium or sodium amide, and dimetallation was only achieved under forced conditions [7]. In order to gain more insight into the polymetallation reaction, we monitored the lithiation by ^7Li NMR spectroscopy.

Appearance of a single peak at 1.7 ppm was observed when one equivalent of C_4H_9Li was added to I. After addition of two equivalents, two peaks appeared, at 1.7 and 2.0 ppm, in a 1/1 intensity ratio; but after addition of three equivalents, only one peak, at 2.0 ppm, was evident. There was no indication of unreacted C_4H_9Li (δ 2.2 ppm), and on the assumption that the signals due to mono-, di- and tri-substituted products do not coincide, we conclude that the distribution is not random, and the formation of VI is favored. Thus crystals of VI separated from a 2/1 mixture of C_4H_9Li and I upon standing for 24 h and at the same time the NMR peak at 2.0 ppm, which is attributed to VI, grew and that at 1.7 ppm vanished. The species giving rise to the signal at 1.7 ppm could not be identified.

Metallation of II is accompanied by the appearance of a single peak at 1.8 ppm, which is not affected by addition of C_4H_9Li. Unless peaks due to partially lithiated species are coincident with that of VII, we can conclude that VII is formed selectively.

Various metallated species were detected during the lithiation of III. With one equivalent of C_4H_9Li, peaks were observed at 1.5, 1.9 and 2.2 ppm, in 1/3/1 ratio. After addition of two equivalents of C_4H_9Li, the ratio changed to 1/1/6, and only the peak at 2.2 ppm, which is assigned to VIII, remained after addition of the third equivalent. Thus formation of the trilithiated species seems to be preferred in each case, and this preference may perhaps be related in the nature of the various molecular structures. Thus, although the solid state structures might well differ from those in solution, we decided to study the crystal and molecular structures of VI, VII and VIII by X-ray diffraction. The results are described below.

Properties

Compounds VI to VIII are colourless crystalline solids soluble in aliphatic and aromatic hydrocarbons. They are decomposed by moisture, though their sensitivity towards H_2O is not very high. Their thermal stability is surprising; they melt without decomposition at 250°C and can be sublimed in vacuo. ^1H and ^7Li NMR parameters are set out in Table 2. The IR and Raman spectra (see Experimental) indicate the absence of any NH groups, and the shift of ν_{as}(SiNSi) (Table 2) to higher frequencies is consistent with earlier observations [11].

X-ray structural determinations

Crystals of VI, VII and VIII were sealed in thin-walled glass capillaries under argon. The space groups were determined from the symmetry and systematic

TABLE 2

PROPERTIES OF COMPOUNDS VI TO VIII

	VI	VII	VIII
Subl. p. (°C/Torr)	$175/10^{-3}$	$155/10^{-3}$	$200/10^{-3}$
^{1}H NMR [a]			
$\delta(SiMe_3)$ (ppm)	0.17	0.27	0.13
δ(R) (ppm)	0.55	1.22	7.96/7.26
^{7}Li NMR [b] (ppm)	2.0	1.8	2.2
ν_{as}(SiNSi) (cm^{-1})	1006	1013	1016

[a] In C_6D_6, int. std. TMS. [b] In n-hexane, ext. std. LiI/H_2O.

absences revealed by Weissenberg photographs. The crystal data in Table 3 were obtained at room temperature with a Siemens AED 1 diffractometer using Zr-filtered Mo-K_α radiation, λ(Mo-$K_{\bar{\alpha}}$) 0.71073 Å. Intensity data were gathered by the ω–2θ

TABLE 3

CRYSTAL DATA AND DETAILS OF THE REFINEMENTS

Compound	VI	VII	VIII
Formula	$C_{20}H_{60}Li_6N_6Si_8$	$C_{26}H_{72}Li_6N_6Si_8$ [a]	$C_{30}H_{64}Li_6N_6Si_8$
M	651.1	735.3 [a]	775.2
Crystal system	tetragonal	cubic	monoclinic
Systematic absences	hkl, $h+k+l \neq 2n$ hhl, $2h+l \neq 4n$ $hk0$, $h(k) \neq 2n$ $0kl$, $k(l) \neq 2n$	$hk0$, $k \neq 2n$	$0k0$, $k \neq 2n$ $h0l$, $l \neq 2n$
Space group	$I4_1/acd$	$Pb3$ [b]	$P2_1/c$
a(Å)	25.801(5)	17.477(3)	10.740(1)
b(Å)			17.890(2)
c(Å)	25.909(6)		13.156(2)
β(°)			108.425(9)
Z	16	4	2
D_x(g/cm^3)	1.00	0.91 [a]	1.07
2θ-limits (°)	3–50	4–55 [b]	2–50
Steps	54–60	51–60	55–62
Step time (s)	0.61	0.61	0.5
Max. step time (s)	1.22	1.22	1.5
Standards variation	0.991–1.006	0.999–1.003	0.997–1.006
Crystal shape	cube	octahedron	parallelepipoid
Crystal size (mm)	0.35	0.28	0.33×0.68×0.79
μ (cm^{-1})	3.2	2.7	5.9
Transmission	0.89–0.91	0.92–0.96	0.55–0.85
Unique reflections	3798	2047	4209
with $F \geq 4\sigma(F)$	1723	762	3381
R [c]	0.099	0.099	0.068
R_w [c]	0.120	0.115	0.098
Final $\Delta\rho$ (e/Å^3)	0.3– –0.39	0.50– –0.23	0.88– –0.50

[a] Ignoring solvent. [b] Non-standard setting of $Pa3$ with equivalent positions x,y,z; $0.5-x$, $0.5+y$, $-z$; $0.5+x$, $-y$, $0.5-z$; $-x$,$0.5-y$,$0.5+z$; z,x,y; $0.5+z$, $-x$,$0.5-y$; $-z$,$0.5-x$,$0.5+y$; $0.5-z$,$0.5+x$, $-y$; y,z,x; $-y$,$0.5-z$,$0.5+x$; $0.5-y$,$0.5+z$, $-x$; $0.5+y$, $-z$,$0.5-x$ plus twelve inversion related positions. [c] $R = \Sigma\Delta/\Sigma|F_0|$ and $R_w = [\Sigma w\Delta^2/\Sigma wF_0^2]^{1/2}$ where $\Delta = ||F_0|-|F_c||$ and $F \geq 4\sigma(F)$.

TABLE 4

POSITIONAL AND EQUIVALENT ISOTROPIC THERMAL PARAMETERS [a] FOR VI

Atom	x	y	z	U
Si(1)	0.2991(1)	0.2034(1)	0.2071(1)	0.053(1)
Si(2)	0.3965(1)	0.2606(1)	0.2510(1)	0.071(1)
Si(3)	0.2563(1)	0.1036(1)	0.2608(1)	0.071(1)
Si(4)	0.2475(1)	0.2405(1)	0.1043(1)	0.082(1)
N(1)	0.3323(3)	0.2488(3)	0.2445(3)	0.056(3)
N(2)	0.2617(3)	0.1683(3)	0.2495(3)	0.060(3)
N(3)	0.2559(3)	0.2371(3)	0.1694(2)	0.057(3)
C(1)	0.4020(4)	0.3162(5)	0.2968(5)	0.125(6)
C(2)	0.4289(4)	0.2833(5)	0.1916(5)	0.117(6)
C(3)	0.4337(4)	0.2050(5)	0.2783(5)	0.130(7)
C(4)	0.3161(5)	0.0727(4)	0.2848(5)	0.123(6)
C(5)	0.2323(5)	0.0663(4)	0.2041(5)	0.117(6)
C(6)	0.2082(5)	0.0940(4)	0.3120(5)	0.134(7)
C(7)	0.2269(5)	0.1776(5)	0.0758(4)	0.123(6)
C(8)	0.3033(5)	0.2654(6)	0.0684(4)	0.152(8)
C(9)	0.1939(6)	0.2874(5)	0.0933(5)	0.165(9)
C(10)	0.3434(4)	0.1619(4)	0.1671(4)	0.086(4)
Li(1)	0.2027(6)	0.1991(7)	0.2079(6)	0.078(7)
Li(2)	0.2939(5)	0.3009(5)	0.2009(5)	0.052(5)
Li(3)	0.1995(6)	0.2871(6)	0.1954(6)	0.064(6)

[a] $U = \frac{1}{3}\Sigma_i\Sigma_j U_{ij} a_i^* a_j^* \bar{a}_i \cdot \bar{a}_j$.

step scan technique, $\Delta\omega$ 0.02°. The number of steps was chosen so that the peaks fell in the middle two-thirds of the scan range. If the intensity of a reflection was found to lie between 2 and 25 $\sigma(I)$, then the scan was repeated and the results accumulated until either this condition was no longer satisfied or the maximum time per step was exceeded. In each case three reflections were monitored every hour in order to check on crystal and instrumental stability. The data were corrected for Lorentz and polarization effects, fluctuation of the standards, and absorption (Table 3).

The structures were solved by direct methods and refined by full-matrix least-

(Continued on p. 313)

TABLE 5

POSITIONAL AND EQUIVALENT ISOTROPIC THERMAL PARAMETERS [a] FOR VII

Atom	x	y	z	U
Si(1)	0.0708(1)	0.0708(1)	0.0708(1)	0.0754(7)
Si(2)	0.1260(2)	−0.0871(2)	0.1491(2)	0.141(2)
N	0.0795(3)	−0.0254(3)	0.0907(3)	0.080(2)
C(1)	0.0952(8)	−0.1865(6)	0.1260(7)	0.198(7)
C(2)	0.2350(9)	−0.088(1)	0.140(1)	0.29(1)
C(3)	0.102(1)	−0.0801(8)	0.2533(6)	0.24(1)
C(4)	0.1344(5)	0.1344(5)	0.1344(5)	0.142(4)
C(5)	0.2202(7)	0.112(1)	0.123(1)	0.25(1)
Li	0.0202(7)	−0.1137(6)	0.0318(7)	0.087(5)
C(6)	0.454(3)	0.454(3)	0.454(3)	0.30(3)
C(7)	0.444(4)	0.460(3)	0.536(3)	0.33(3)

[a] See Table 4.

TABLE 6

POSITIONAL AND EQUIVALENT ISOTROPIC THERMAL PARAMETERS [a] FOR VIII

Atom	x	y	z	U
Si(1)	0.63466(9)	−0.02438(5)	0.15061(7)	0.0446(3)
Si(2)	0.3898(1)	−0.03186(6)	0.24069(9)	0.0599(4)
Si(3)	0.7170(1)	−0.17072(5)	0.04923(8)	0.0515(4)
Si(4)	0.76895(9)	0.13305(6)	0.15414(9)	0.0564(4)
N(1)	0.4750(3)	−0.0229(1)	0.1531(2)	0.046(1)
N(2)	0.6406(3)	−0.0890(1)	0.0537(2)	0.0462(9)
N(3)	0.6634(3)	0.0622(1)	0.1026(2)	0.048(1)
C(1)	0.4093(6)	−0.1223(3)	0.3139(5)	0.110(3)
C(2)	0.4171(8)	0.0436(3)	0.3429(4)	0.128(4)
C(3)	0.2093(6)	−0.0250(4)	0.1591(5)	0.128(4)
C(4)	0.8983(5)	−0.1654(3)	0.0677(6)	0.109(3)
C(5)	0.6437(5)	−0.2077(3)	−0.0917(4)	0.086(2)
C(6)	0.6914(7)	−0.2429(3)	0.1407(5)	0.111(3)
C(7)	0.7325(5)	0.2090(3)	0.0504(4)	0.091(2)
C(8)	0.9462(5)	0.1098(4)	0.1832(6)	0.124(3)
C(9)	0.7489(6)	0.1738(3)	0.2780(4)	0.098(2)
C(10)	0.7606(4)	−0.0491(2)	0.2841(3)	0.068(2)
C(11)	0.7421(7)	−0.0596(5)	0.3746(5)	0.154(4)
C(12)	0.8396(8)	−0.0851(7)	0.4684(7)	0.186(6)
C(13)	0.947(1)	−0.0981(5)	0.4687(7)	0.168(5)
C(14)	0.9868(9)	−0.0892(6)	0.3769(7)	0.182(5)
C(15)	0.8898(7)	−0.0636(4)	0.2852(5)	0.146(3)
Li(1)	0.4498(6)	−0.1077(3)	0.0456(5)	0.054(2)
Li(2)	0.6910(6)	0.0004(3)	−0.0161(5)	0.055(2)
Li(3)	0.4789(6)	0.0859(3)	0.1065(5)	0.055(2)

[a] See Table 4.

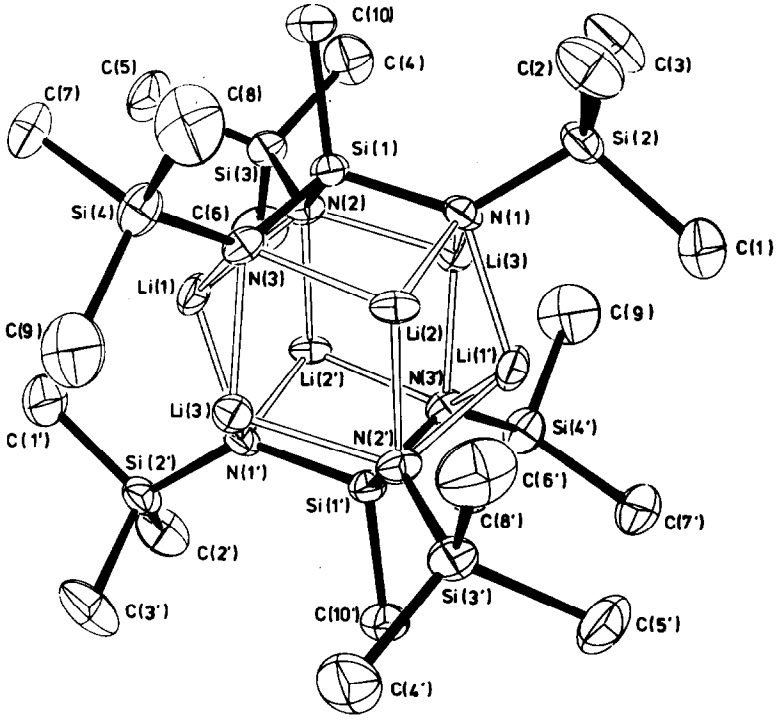

Fig. 1. A perspective drawing of VI.

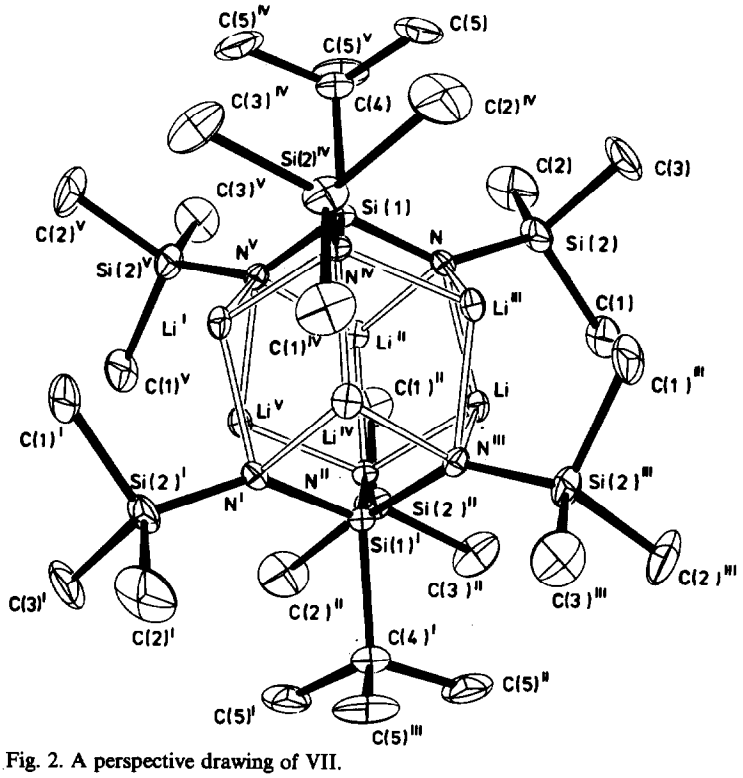

Fig. 2. A perspective drawing of VII.

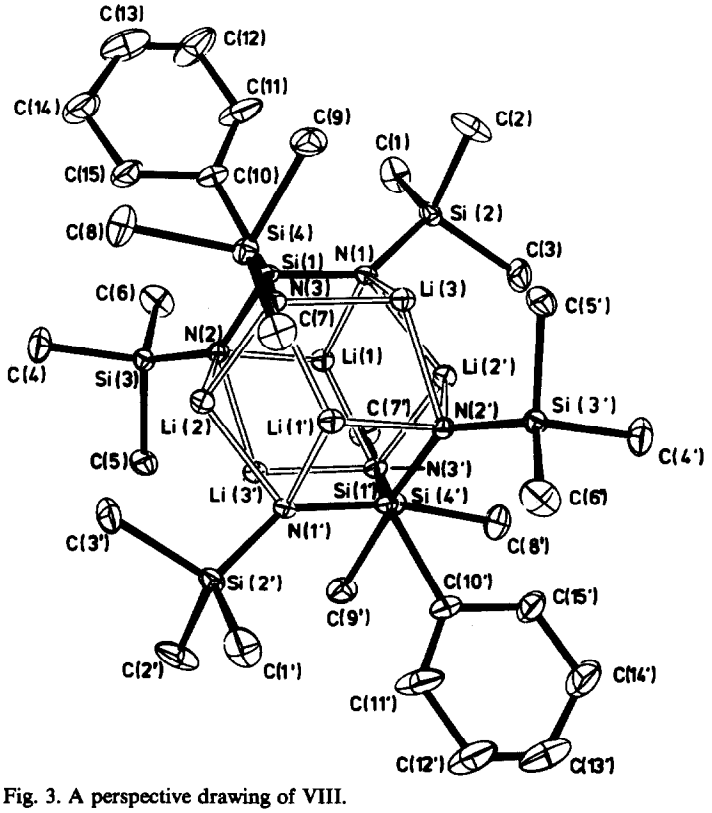

Fig. 3. A perspective drawing of VIII.

squares techniques using the SHELX-76 program [12]. Dispersion corrected scattering factors [13] were used for all atoms. Only those reflections with $|F_0| \geq 4\sigma(|F_0|)$ were used in the refinements, the weights being defined by $w^{-1} = \sigma^2(|F_0|) + 0.0009|F_0|^2$.

After anisotropic refinement of the C, Li, N and Si atoms, H atoms were placed in ideal positions (C–H 0.95 Å, with phenyl hydrogens on bisectors of the C–C–C angles and methyl hydrogen in staggered conformations with H–C–H 109.5°). Difference Fourier syntheses showed positive electron density at these locations. The H atoms were allowed to ride on their respective C atoms and were assigned group isotropic temperature factors. Convergence was reached in each case, $|\xi/\sigma|_{max} = 0.50$.

Crystals of VII contain large cavities of $\bar{3}$ site symmetry, which apparently contain disordered solvent molecules. Coordinates of two peaks found in a difference Fourier map were assigned C-atom form factors. They were refined isotropically along with a common occupancy factor.

The final difference syntheses of VI and VII are featureless. That of VIII contains four peaks (0.4–0.9 e/Å^3) near the phenyl ring in an otherwise flat map.

The residuals and other details of the refinements are given in Table 3. Fractional

TABLE 7

SELECTED DISTANCES (Å) IN VI, VII AND VIII

A(i)–A(j) [a]	VI	A(j)	VII	A(j)	VIII
Si(1)–N(1)	1.746(7)	N	1.723(5)	N(1)	1.726(3)
Si(1)–N(2)	1.721(8)			N(2)	1.737(3)
Si(1)–N(3)	1.718(7)			N(3)	1.737(3)
Si(2)–N(1)	1.693(8)	N	1.692(6)	N(1)	1.691(3)
Si(3)–N(2)	1.703(8)			N(2)	1.687(3)
Si(4)–N(3)	1.704(7)			N(3)	1.693(3)
N(1)–Li(1') [b]	2.03(2)	Li	2.13(1)	Li(2')	2.134(7)
N(2)–Li(2') [b]	2.08(2)			Li(3')	2.092(6)
N(3)–Li(3) [b]	2.06(2)			Li(1')	2.107(6)
N(1)–Li(2)	2.02(2)	Li''	1.99(1)	Li(1)	2.032(6)
N(1)–Li(3')	1.99(2)	Li'''	2.03(1)	Li(3)	2.045(6)
N(2)–Li(1)	2.03(2)			Li(1)	2.046(7)
N(2)–Li(3')	2.09(2)			Li(2)	2.001(7)
N(3)–Li(1)	1.96(2)			Li(2)	2.010(7)
N(3)–Li(2)	2.08(2)			Li(3)	2.043(7)
Li(1)–Li(2')	2.36(2)	Li''	2.35(2)	Li(2')	2.398(9)
Li(1)–Li(3)	2.29(2)	Li'''	2.35(2)	Li(3')	2.389(9)
Li(2)–Li(3)	2.47(2)			Li(3')	2.398(9)
Si(1)–Li(1)	2.49(2)	Li'	2.51(1)	Li(1)	2.517(6)
Si(1)–Li(2)	2.53(1)			Li(2)	2.492(6)
Si(1)–Li(3')	2.54(2)			Li(3)	2.532(6)
Li(1)–C(1')	2.73(2)	C(1)	2.46(2)	C(7')	2.674(8)
Li(2)–C(6')	2.73(2)			C(3')	2.480(9)
Li(3)–C(9)	2.65(2)			C(5')	2.522(8)
Si(1)–C(10)	1.88(1)	C(4)	1.92(2)	C(10)	1.899(4)

[a] Primed atoms are related to those in the asymmetric units by $x', y', z' = 0.5 - x, 0.5 - y, 0.5 - z$ for VI, by $x', y', z' = -x, -y, -z$, $x'', y'', z'' = -z, -x, -y$ and $x''', y''' z''' = -y, -z, -x$ for VII and $x', y', z' = 1 - x, -y, -z$ for VIII. [b] These N–Li bonds lie in the molecular mirror planes.

coordinates of the nonhydrogen atoms are listed in Tables 4, 5 and 6, and the numbering schemes are defined in the ORTEP plots [14] shown in Figs. 1, 2 and 3 *.

Description of the crystal structures

Compounds VI, VII and VIII were shown to crystallize as discrete, dimeric species. Molecules of VI and VIII are centered on sites of crystallographic $\bar{1}$ (C_i) symmetry, while the crystallographic symmetry of VII is higher, $\bar{3}$ (S_6).

The cores of the dimers contain six Li atoms, each six defining the corners of a trigonal antiprism. Each pair of tripod ligands is so disposed about the Li_6 clusters that each SiN_3 fragment is centered over a trigonal face, with the N atoms staggered with respect to the Li atoms in this face. Thus the symmetry of the $(SiN_3Li_3)_2$ clusters approaches $\bar{3}m$ (D_{3d}). Bond distances and angles (Tables 7 and 8, respectively) reflect this symmetry closely. Even each $SiMe_3$ moiety is so oriented that one Me group lies, on the average, 0.08(6) Å from a diagonal mirror plane, and the Me(t-Bu) groups in VI are displaced only 0.04(2) Å from one of the three mirror planes.

Each N atom is bonded to three Li and two Si atoms, and is thus pentacoordinate. Since a N atom can have only four electron pairs in its valence shell, electron-deficient bonding must be present in VI, VII and VIII. The first silylamide structure shown to possess pentacoordinate N atoms was $Me_2Si(NaNSiMe_3)_2$ [7], and N pentacoordination has also been suggested, albeit more equivocally, for $(LiNC\text{-}t\text{-}Bu_2)_6$ and $[LiNC(NMe_2)_2]_6$ [15]. The Li(cn3)–N(cn5) distances average 2.06(1) and 2.00(1) Å, respectively, in the last two compounds, and are similar to

TABLE 8

SELECTED BOND ANGLES (°) IN VI, VII AND VIII

A(i)-A(j)-A(k)	VI	A(k)	VII	A(k)	VIII
Si(1)–N(1)–Si(2)	131.0(5)	Si(2)	141.8(4)	Si(2)	140.1(2)
Si(1)–N(2)–Si(3)	132.2(5)			Si(3)	137.2(2)
Si(1)–N(3)–Si(4)	132.1(4)			Si(4)	134.1(2)
N(1)–Si(1)–C(10)	113.0(4)	C(4)	113.3(2)	C(10)	114.1(2)
N(2)–Si(1)–C(10)	113.2(4)			C(10)	110.0(2)
N(3)–Si(1)–C(10)	111.8(4)			C(10)	112.8(2)
N(1)–Si(2)–C(1) [a]	106.0(4)	C(1)	109.0(4)	C(3)	106.5(2)
N(2)–Si(3)–C(6) [a]	108.1(4)			C(5)	106.3(2)
N(3)–Si(4)–C(9) [a]	106.2(5)			C(7)	107.0(2)
N(1)–Si(2)–C(2)	114.6(4)	C(2)	115.7(6)	C(1)	116.0(2)
N(1)–Si(2)–C(3)	113.8(5)	C(3)	116.0(5)	C(2)	115.3(3)
N(2)–Si(3)–C(4)	114.4(5)			C(4)	116.4(2)
N(2)–Si(3)–C(5)	113.5(4)			C(6)	114.2(2)
N(3)–Si(4)–C(7)	112.6(5)			C(8)	115.2(3)
N(3)–Si(4)–C(8)	115.0(5)			C(9)	113.4(2)

[a] These N–Si–C bond angles lie in the molecular mirror planes.

* F_o, F_c lists, tables of hydrogen coordinates and anisotropic thermal parameters may be obtained from Fachinformationszentrum Energie Physik Mathematik, D-7514 Eggenstein-Leopoldshafen, by quoting the deposit number CSD 51145, the names of the authors and the literature references.

those in VI, VII and VIII, mean 2.05(5) Å. In the present study, however, the Li–N bond lengths may be grouped into two categories. Those bonds lying in the diagonal mirror planes (mean 2.10(3) Å) tend to be longer than those inclined to these planes (mean 2.02(3) Å). The other known Li–N distances in unsolvated lithium silylamides come from investigations of $[LiN(SiMe_3)_2]_n$, which contain two-coordinate Li and four-coordinate N atoms, the distance being 1.99(3) Å in the gas phase ($n = 2$) [3c] and 2.00(2) Å in the solid state ($n = 3$) [3a,b].

The Si–N bond lengths involving the central Si atoms, mean 1.728(9) Å, are significantly longer than those formed by the $SiMe_3$ groups, mean 1.694(6) Å. The latter value is shorter than those reported for $[LiN(SiMe_3)_2]_n$, 1.712(7) and 1.729(4) Å for $n = 2$ [3c] and 3 [3a,b], respectively. Considerable variation is found for the Si–N–Si angles, which are smallest in VI (mean 131.8(7)°), and largest in VII (141.8(4)°), and range from 134.1(2) to 140.1(2)° in VIII. Since the Si–C(10) and N–Si($SiMe_3$) bonds are essentially eclipsed (moduli of the C(10)–Si(1)–N–Si torsion angles average 3(3)°), the Si–N–Si angles might well be opened by steric repulsions between RSi and $SiMe_3$ groups. Thus, as expected, the smallest angles are observed for VI (R = Me) and the widest for VII (R = t-Bu). For VIII the steric factor should be greatest for the N(1)–Si(2) bond, because only this bond lies close to the plane of the phenyl ring; the Si(1)–N(1)–Si(2) angle is, in fact, the largest in VIII. Smaller angles were reported for other unsolvated lithium silylamides; e.g. in $[LiN(SiMe_3)_2]_n$, values of 130(2) and 118.6(9)° were found for $n = 2$ and $n = 3$, respectively.

Before additional evidence for structurally significant RSi, $SiMe_3$ steric interactions can be evaluated, it should be noted that each $SiMe_3$ group is so oriented that one of the three Si(1)–N–Si–C fragments adopts a *trans* conformation. (The only other conformation which would preserve the $\bar{3}m$ symmetry requires a *cis* conformation of one of the three Si(1)–N–Si–C moieties; such a conformation is probably energetically unfavorable, and has not been observed.) In accord with the steric model, the N–Si–C angles involving C atoms which belong to Si(1)–N–Si–C fragments displaying a *gauche* conformation, and are thus closest to the RSi group, are somewhat smaller for VI (114.0(9)°) than for VII (115.8(3)°) and intermediate for VIII (115(1)°).

However, since the spread in these average angles is barely 2°, steric effects alone may not account for the mean of the remaining N–Si–C angles being 8° smaller, 107(1)°. The Me groups involved in the latter valencies are those associated with the diagonal mirror planes, and each is positioned near one of the Li atoms. The Me, Li contacts vary from 2.46(2)–2.73(2) Å. These contacts are shortest when the Si–N–Si angles are largest (e.g., 2.46(2) Å in VII and 2.71(5) in VI), and the shortest are comparable to the shortest Li–C contacts between tetramers in $(EtLi)_4$, 2.502(2) Å [16].

The geometry assumed for the Me groups requires that each Li...C interaction be accompanied by two Li...H contacts of 2.20–2.54 Å. Shorter such contacts were reported in $LiBMe_4$, 2.116(9) Å [17].

Unfortunately, the large torsional motions of the $SiMe_3$ groups preclude a direct determination of the H atom positions in the present structures and probably also prevent refinement to lower R values. In particular, the generally large thermal disorder in VII is undoubtedly related to the fact that the molecular packing leaves cavities large enough to contain disordered solvent. (Samples used for the elemental analyses were previously dried in vacuo and so contained no included solvent.)

TABLE 9

COMPARISON OF VARIOUS Li_6B_6 POLYHEDRA

Structure	θ(Li) [a]	θ(B) [a]	r(Li) [b]	r(B) [b]	Li...B [c]	Li...Li [c]	N...N [c]
Icosahedron	79.19	37.38	r	r	1.051r/1.00	1.051r/1.00	1.051r/1.00
VI [d]	73.6(2)	48.6(1)	2.13(3)	2.125(6)	2.04(5)/0.91	2.37(9)/1.06	2.76(3)/1.24
VII [d]	72.7(3)	47.3(6)	2.09(1)	2.154(5)	2.05(7)/0.92	2.35(1)/1.07	2.740(9)/1.21
VIII [d]	72.9(2)	48.1(1)	2.134(6)	2.154(3)	2.06(5)/0.91	2.395(9)/1.07	2.777(5)/1.23
$[LiNC(NMe_2)_2]_6$ [e]	66.1(4)	59.8(1)	2.00(3)	2.38(2)	2.00(1)/0.87	2.445(4)/1.16	3.57(3)/1.42
$[LiC_6H_{11}]_6$ [f]	64.0(1)	60.0(1)	1.907(7)	2.74(1)	2.22(6)/0.91	2.40(1)/1.20	4.104(7)/1.43
$[LiSiMe_3]_6$ [g]	62.4(2)	61.9(8)	2.12(2)	3.34(3)	2.69(6)/0.94	2.71(2)/1.22	5.10(2)/1.45

[a] Azimuthal angles (°). [b] Radial distances (Å). [c] Observed edge lengths (Å)/observed length divided by predicted icosahedral value. [d] Present study, B = N. [e] Ref. 15, B = N. [f] Ref. 23, B = C. [g] Ref. 18, B = Si.

Each central Si atom is involved three unusually short Si...Li contacts (mean 2.51(2) Å) with Li atoms of a trigonal face of a Li_6 antiprism. These distances are even shorter than the mean bonding Si–Li contacts in $[LiSiMe_3]_6$, 2.69(6) Å [18], and $[Me_3SiLi(TMEDA)]_2TMEDA$, 2.70(1) Å [19]. However, if these Si...Li contacts in the present study were bonding, then the N–Si–C angles at the central Si atoms might have been expected to be smaller than those observed, mean 113(1)°. Since the edges of the non-trigonal faces of the Li_6 antiprisms in VI, VII and VIII (mean 2.37(5) Å) are about as long as these short Si...Li contacts, a "cubic" arrangement of the Li_6Si_2 fragment is apparent. Thus an alternative description of the clusters is that of a Li_6Si_2 cube omni-capped by six $NSiMe_3$ groups. To our knowledge, the only other example of such a 14 vertex polyhedral structure was encountered in an unusual side-on μ-N_2 complex [20], although such structures have been considered as possible candidates for $B_{14}H_{14}^{2-}$ [21].

Discussion

The similarity of the structures found for VI, VII and VIII implies that these dimers are the favored mode of aggregation of $RSi(LiNSiMe_3)_3$ compounds and so a detailed analysis of the Li_6N_6 cluster seems appropriate. While closest packing of twelve equivalent atoms is achieved with an icosahedral arrangement, several factors cause the Li_6N_6 fragment to be distorted from this arrangement. First, the equivalence criterion is obviously not fulfilled, and by placing the N atoms at the corners of two transoid faces of an icosahedron and the Li atoms at the other vertices, the cluster symmetry is reduced to that observed in this study, $\bar{3}m$. Secondly, use of twelve pairs of electrons in the Li_6N_6 cluster bonding would leave the degenerate HOMO for an icosahedral structure partially filled [22].

In order to compare structures of $\bar{3}m$ symmetry to an icosahedron, we define the radial coordinates r(Li) and r(N), which are the distances of the respective atoms from the center of the polyhedron, and the azimuthal angles, θ(Li) and θ(N), which are formed by vectors in the r(Li) and r(N) direction, respectively, and the threefold axis. The length l of an icosahedral edge is then related to the radial coordinate r by equation 1, and so the influence of the azimuthal distortions on the Li...Li and N...N contacts can be readily appreciated. Furthermore, the Li–N distances may be compared with the mean of the predictions for the "undistorted" Li...Li and N...N contacts. These comparisons are made in Table 9.

With respect to icosahedral values, θ(Li) and θ(N) are changed in such a way as to decrease the separation between N_3 and Li_3

$$l = r/\left[\frac{1}{4} + \frac{1}{(\sqrt{5}-1)^2}\right]^{1/2} \quad (1)$$

layers along the threefold axis, lengthen the distance between the two Li_3 layers, and widen the N_3 faces. These distortions reduce the Li–N edges by ~ 9%, while the Li–Li and N–N edges are increased by ~ 7 and ~ 23%, respectively. A straightforward interpretation of these differences is that the Li–N interactions stabilize the cluster whereas Li...Li and, to a greater extent, N...N contacts, are destabilizing. While the analysis of the Li–N bonding seems trivial, differentiation between Li...Li and N...N interactions is not.

Examination of the radial and azimuthal parameters (Table 9) for $[LiNC(NMe_2)_2]_6$ is also instructive. When the atoms of an N_3 face are not bonded to the same Si atom, the difference between r(Li) and r(N) becomes distinct, and greater deviations from icosahedral values are displayed by both θ(Li) and θ(N). Interestingly, the latter angles are similar to the values calculated from the coordinates reported for the hexamer of cyclohexyllithium [23] and $[LiSiMe_3]_6$ [18], for which even greater divergences in the radial parameters are obtained. Compared to lengths predicted for the icosahedral edges, however, the same bond shortening and lengthening features are found in the latter three compounds as in VI, VII and VIII. Thus the model developed here appears to be quite useful when a A_6B_6 cluster of $\bar{3}m$ symmetry is to be related to its icosahedral parent.

Experimental

Synthesis

Compound III was prepared as described in ref. 10 and t-$BuSiCl_3$ as described in ref. 24.

Methyltris(trimethylsilylamino)silane (I). (a) A mixture of 78 g (0.52 mol) $MeSiCl_3$, 253 g (1.57 mol) $(Me_3Si)_2NH$ and 82 g (1 mol) C_5H_5N is kept at 120°C for 8 h. Me_3SiCl, pyridine, and residual $(Me_3Si)_2NH$ are distilled off, and the residue is fractionated in vacuo through a 30 cm Vigreux column, yield 13 g (17%).

(b) A solution of 180 g (1.65 mol) Me_3SiCl and 75 g (0.5 mol) $MeSiCl_3$ in 3 l petroleum ether is saturated with gaseous ammonia at 0°C, NH_4Cl is filtered off, the solvent evaporated, and the residue distilled in vacuo; yield 8.2 g (5%). For analysis see Table 10.

t-Butyltrimethylsilylamino-dichlorosilane (IV). A mixture of 38.3 g (0.2 mol) t-$BuSiCl_3$, 97 g (0.6 mol) $(Me_3Si)_2NH$, and 36 g (0.45 mol) C_5H_5N is kept at 140°C for 8 h and worked up as described for I, method (a). Yield 7.4 g (13%).

t-Butylbis(trimethylsilylamino)aminosilane (V). A solution of 19.4 g (0.1 mol)

TABLE 10

ANALYSES

	Sum formula	Analyses (Found (calcd.) (%))				
		C	H	Cl	Li	N
I	$C_{10}H_{33}N_3Si_4$					13.3 (13.65)
II	$C_{13}H_{39}N_3Si_4$					12.0 (12.01)
IV	$C_7H_{19}Cl_2NSi_2$			29.1 (29.02)		5.5 (5.73)
V	$C_{10}H_{31}N_3Si_3$					14.9 (15.13)
VI	$C_{10}H_{30}Li_3N_3Si_4$				6.3 (6.39)	12.7 (12.91)
VII	$C_{13}H_{36}Li_3N_3Si_4$				5.4 (5.66)	11.1 (11.44)
VIII	$C_{15}H_{32}Li_3N_3Si_4$	46.5 (46.48)	8.1 (8.32)		5.3 (5.37)	10.8 (10.84)

t-$BuSiCl_3$ and 33 g (0.3 mol) Me_3SiCl in 800 ml petrol ether is saturated with gaseous ammonia at 0°C. The NH_4Cl is filtered off, the filtrate evaporated, and the residue distilled in vacuo, yield 4.2 g (15%).

t-Butyltris(trimethylsilylamino)silane (III). 15 g (0.054 mol) V in 100 ml petroleum ether and 10 ml THF is metallated with C_4H_9Li in hexane, then 5.9 g (0.054 mol) Me_3SiCl added. The mixture is stirred for 20 h the LiCl is filtered off, the solvent evaporated, and the residue distilled in vacuo; yield 13.2 (70%).

Methyltris(trimethylsilyl-N-lithioamino)silane (VI). 3.6 g (12 mmol) I in 7 ml petroleum ether are metallated with a stochiometric amount of C_4H_9Li in n-hexane. A precipitate is formed. The mixture is cooled to −25°C and the precipitate collected, yield 2.0 g (53%). Analogous: t-Butyltris(trimethylsilyl-*N*-lithioamino)silane VII, yield 57%, and phenyltris(trimethylsilyl-*N*-lithioamino)silane VIII, yield 62%.

Spectra

Raman spectra were obtained of neat liquids or crystalline material in 1 mm ∅ capillaries with a Cary 82 instrument, excitation Kr^+ 6471 Å, wavenumber accuracy ± 2 cm^{-1}. IR spectra were measured of neat liquids or Nujol mulls (VI to VIII) with a Perkin–Elmer 580B spectrometer, wavenumber accuracy ± 2 cm^{-1}.

I: Raman 156w, 172s, 225m, 246vw, 302w, 550vs, 632vs, 683m, 721w, 752vw, 835w, 1256w, 1408m, 2898vs, 2957m, 3383m. IR 439s, 560w, 599s, 634m, 682vs, 721m, 752sh, 768sh, 782s, 833vs, 919vs, 1178vs, 1252vs, 1411s, 1439w, 2897vs, 2958vs, 3385vs.

II: Raman 129m, 162w, 196w, 208s, 275w, 309w, 476m, 545vs, 613w, 651vs, 684m, 761w, 820m, 937m, 1005vw, 1183w, 1214w, 1257w, 1409m, 1443w, 1462m. IR 350s, 435m, 471vs, 542s, 609vs, 653w, 687vs, 770vs, 837vs, 869vs, 933vs, 1008m, 1063m, 1177vs, 1250vs, 1337sh, 1360s, 1399w, 1413m, 1444vw, 1468sh, 1475vs, 2849vs, 2898vs, 2938vs, 2960vs, 3380vs.

IV: Raman 130m, 167m, 187w, 212m, 297s, 399w, 470vs, 564w, 604vs, 633m, 690m, 765w, 824s, 942w, 1188vw, 1213m, 1261vw, 2867w, 2897w, 2924vw, 2954w. IR 360s, 411vs, 475vs, 559vs, 600m, 630s, 688s, 766s, 826sh, 862vs, 952vs, 1010w, 1089w, 1180vs, 1191sh, 1218vw, 1255vs, 1294w, 1368s, 1398m, 1415m, 1467s, 1476s, 2864s, 2901m, 2922sh, 2960vs, 3373s.

V: Raman 210s, 293w, 572vs, 657m, 685m, 759w, 826s, 939m, 1009vw, 1185w, 1218m, 1257w, 1411w, 1445m, 1463m, 2854s, 2893vs, 2920sh, 2950s. IR 451s, 575sh, 604s, 682s, 764s, 836s, 876vs, 934vs, 1007m, 1080m, 1178vs, 1249vs, 1361s, 1390m, 1411w, 1446vw, 1469sh, 1473s, 1542s, 2858s, 2897m, 2950vw, 2996vs, 3385s, 3461s, 3495s.

VI: Raman 165vw, 193s, 220w, 248m, 338s, 455s, 588vs, 618s, 661s, 827m, 1410m. IR 430vw, 446vw, 463w, 501m, 617sh, 658w, 723s, 743vw, 751vw, 771s, 836vs, 1006vs, 1249vs.

VII: Raman 137m, 193vs, 218vs, 263w, 334w, 358m, 474w, 543s, 614vs, 651w, 669w, 748vw, 820m, 1005vw, 1200m, 1448m, 1460m. IR 433w, 508m, 560sh, 580vs, 615m, 661s, 725sh, 738s, 823vs, 846sh, 1013vs, 1255vs.

VIII: Raman 179s, 211w, 246vw, 326m, 372m, 469vw, 583vs, 656vw, 670m, 734vw, 748vw, 819w, 997s, 1026m, 1411w, 1439vw, 1588w, 2886w, 2937m, 3035w, IR 424w, 501m, 588s, 636vw, 668m, 702m, 739s, 826vs, 851sh, 1016vs, 1108m, 1252vs.

Mass spectra (Varian MAT 311, EI, 70 eV)

I: *m/e* 292 ($M^+ - 15$, 60%), 275 ($M^+ - 2 \times 15$, 67%), 203 ($M^+ - Me_3Si - MeH - 15$, 100%), 187 ($M - Me_3Si - 2MeH - 15$, 11%), 130 ($Me_2SiNSiMe_2^+$, 27%), 73 (Me_3Si^+, 20%).

II: *m/e* 334 ($M^+ - 15$, 12%), 292 ($M^+ - Me_3C$, 96%), 276 ($M^+ - Me_3Si$, 100%), 203 ($M^+ - 2Me_3Si$, 96%), 188 ($M^+ - 2Me_3Si - 15$, 14%), 130 ($Me_2SiNSiMe_2^+$; $M^+ - 3Me_3Si$, 21%), 73 (Me_3Si^+, 10%).

IV: *m/e* 228 ($M^+ - 15$, 2%), 186 ($M^+ - Me_3C$, 100%), 170 ($M^+ - Me_3Si$, 10%), 151 ($M^+ - Me_3C$-Cl, 34%), 73 (Me_3Si^+, 18%), 57 (Me_3C^+, 21%).

V: *m/e* 262 ($M^+ - 15$, 5%), 245 ($M^+ - NH_3 - 15$, 12%), 220 ($M^+ - Me_3C$, 71%), 131 ($M^+ - 2Me_3Si$, 57%), 74 (Me_2SiNH^+, 14%), 73 (Me_3Si^+, 12%).

Acknowledgements

Support by the Fonds der Chemie, and a gift of chemicals by Bayer AG are gratefully acknowledged.

References

1 (a) E. Niecke and R. Rüger, Angew. Chem., 95 (1983) 154; (b) T. Fjeldberg, H. Hope, M.F. Lappert, P.P. Power and A.J. Thorne, J. Chem. Soc. Chem. Commun., (1983) 639.
2 M.F. Lappert, P.P. Power, A.R. Sanger and R.C. Srivastava, Metal and Metalloid Amides, Wiley, Chichester, 1980.
3 (a) D. Mootz, A. Zinnius and B. Böttcher, Angew. Chem., 81 (1969) 398; (b) R.D. Rogers, J.L. Atwood and R. Grüning, J. Organomet. Chem., 157 (1978) 229; (c) T. Fjeldberg, P.B. Hitchcock, M.F. Lappert and A.J. Thorne, J. Chem. Soc. Chem. Commun., (1984) 822; (d) L.M. Engelhardt, A.S. May, C.L. Raston and A.H. White, J. Chem. Soc. Dalton Trans., (1983) 1671; (e) M.F. Lappert, M.J. Slade, A. Single, J.L. Atwood, R.D. Rogers and R. Shakir, J. Amer. Chem. Soc., 105 (1983) 302.
4 P.P. Power and X. Xiaojie, J. Chem. Soc. Chem. Commun., (1984) 358.
5 R. Grüning and J.L. Atwood, J. Organomet. Chem., 137 (1977) 101.
6 A.M. Domingos and G.M. Sheldrick, Acta Crystallogr. B, 30 (1974) 517.
7 D.J. Brauer, H. Bürger, W. Geschwandtner, G.R. Liewald and C. Krüger, J. Organomet. Chem., 248 (1983) 1.
8 D.A. Zhinkin, G.N. Mal'nova and Zh.V. Gorislavskaya, Plasticheskie Massy (1965) 18; Chem. Abstr., 64 (1966) 6677.
9 K.A. Andrianov, G.U. Kotrelev, V.V. Kazakova and I.E. Rogo, Bull. Acad. Sci. U.S.S.R., Div. Chem. Sci., (1975) 2489.
10 E.P. Lebedev and R.G. Valimukhametova, J. Gen. Chem. U.S.S.R., 47 (1977) 978.
11 U. Wannagat, Pure Appl. Chem., 19 (1969) 329.
12 G.M. Sheldrick, SHELX-76: Program for crystal structure determination, University of Cambridge, England, 1976.
13 International Tables for X-ray Crystallography, Vol. IV, Birmingham: Kynoch Press 1974.
14 C.K. Johnson, ORTEP: Report ORNL-3794, Oak Ridge National Laboratory, Tennessee, 1965.
15 W. Clegg, R. Snaith, H.M.M. Shearer, K. Wade and G. Whitehead, J. Chem. Soc. Dalton Trans., (1983) 1309.
16 H. Dietrich, J. Organomet. Chem., 205 (1981) 291.
17 W.E. Rhine, G. Stucky and S.W. Peterson, J. Am. Chem. Soc., 97 (1975) 6401.
18 W.H. Ilsley, T.F. Schaaf, M.D. Glick and J.P. Oliver, J. Am. Chem. Soc., 102 (1980) 3769.
19 B. Teclé, W.H. Ilsley and J.P. Oliver, Organometallics, 1 (1982) 875.
20 K. Jonas, D.J. Brauer, C. Krüger, P.J. Roberts and Y.-H. Tsay, J. Am. Chem. Soc., 98 (1976) 74.
21 L.D. Brown and W.N. Lipscomb, Inorg. Chem., 16 (1977) 2989.
22 H.C. Longuet-Higgins and M. de V. Roberts, Proc. Roy. Soc. A, 230 (1955) 110.
23 R. Zerger, W. Rhine and G. Stucky, J. Am. Chem. Soc., 96 (1974) 6048.
24 L.J. Tyler, L.H. Sommer and F.C. Whitmore, J. Am. Chem. Soc., 70 (1948) 2876.